ELSEVIER

SCIENCE DIRECT®

PHYSICS LETTERS B

Physics Letters B 557 (2003) 45–54

www.elsevier.com/locate/npe

Problems of double-charm production in e^+e^- annihilation at $\sqrt{s} = 10.6$ GeV

Kui-Yong Liu [a], Zhi-Guo He [a], Kuang-Ta Chao [a,b]

[a] *Department of Physics, Peking University, Beijing 100871, PR China*
[b] *China Center of Advanced Science and Technology, World Laboratory, Beijing 100080, PR China*

Received 20 November 2002; received in revised form 23 January 2003; accepted 27 January 2003

Editor: T. Yanagida

Abstract

Using the nonrelativistic QCD (NRQCD) factorization formalism, we calculate the color-singlet cross sections for exclusive production processes $e^+ + e^- \to J/\psi + \eta_c$ and $e^+ + e^- \to J/\psi + \chi_{cJ}$ $(J = 0, 1, 2)$ at the center-of-mass energy $\sqrt{s} =$ 10.6 GeV. The cross sections are estimated to be 5.5 fb, 6.7 fb, 1.1 fb, and 1.6 fb for η_c, χ_{c0}, χ_{c1}, and χ_{c2}, respectively. The calculated $J/\psi + \eta_c$ production rate is smaller than the recent Belle data by about an order of magnitude, which might indicate the failure of perturbative QCD calculation to explain the double-charmonium production data. The complete $\mathcal{O}(\alpha_s^2)$ color-singlet cross section for $e^+ + e^- \to \chi_{c0} + c\bar{c}$ is calculated. In addition, we also evaluate the ratio of exclusive to inclusive production cross sections. The ratio of $J/\psi\eta_c$ production to $J/\psi c\bar{c}$ production could be consistent with the experimental data.

PACS: 12.40.Nn; 13.85.Ni; 14.40.Gx

Heavy quarkonium production is interesting in understanding both perturbative and nonperturbative quantum chromodynamics (QCD). In recent years the charmonium production has been studied in various processes, such as in hadron–hadron collision, electron–proton collision, fixed target experiments, B meson decays, as well as Z^0 decays. Among them, the study of charmonium production in e^+e^- annihilation is particularly interesting in testing the quarkonium production mechanisms, the color-singlet model and the color-octet model in the nonrelativistic QCD (NRQCD) [1] approach. This is not only because of the simpler parton structure involved in this process, which may be helpful in reducing the theoretical uncertainty, but also because of the spectacular experimental prospect opened up by the two B factories with BaBar and Belle, which will allow a fine data analysis for charmonium production with more than 10^8 e^+e^- annihilation events in the continuum at $\sqrt{s} = 10.6$ GeV.

Recently the Belle Collaboration has reported the observation of prompt J/ψ via double $c\bar{c}$ production from the e^+e^- continuum [2]. For these results, not only the large cross section (≈ 0.9 pb) of the inclusive J/ψ production due to the double $c\bar{c}$ is puzzling [3], but also the exclusive production rate of $J/\psi\eta_c$, $\sigma(e^+ + e^- \to J/\psi + \eta_c(\gamma)) \times \mathcal{B}(\eta_c \to \geqslant 4 \text{ charged}) = (0.033^{+0.007}_{-0.006} \pm 0.009)$ pb, may not be consistent with two previous

E-mail address: ktchao@th.phy.pku.edu.cn (K.-T. Chao).

0370-2693/03
doi:10.1016/S0370-2693(03)00176-X

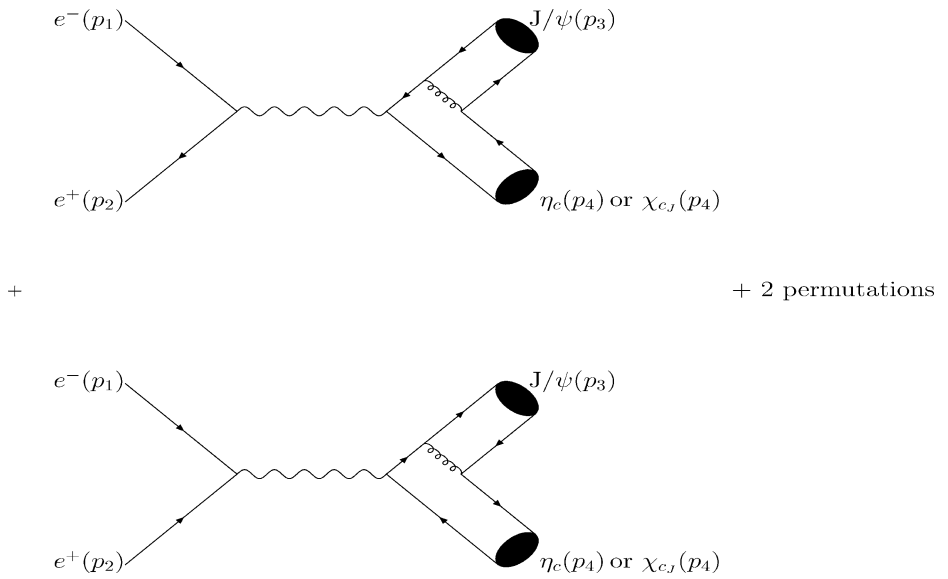

Fig. 1. Feynman diagrams for $e^+e^- \to J/\psi + \eta_c(\chi_{cJ})$.

calculations [4,5], which gave a cross section of a few pb for $J/\psi\eta_c$. In fact, recent perturbative QCD estimates of the $J/\psi c\bar{c}$ cross section are only about $0.1 \sim 0.2$ pb [6–9]. So the calculations of exclusive cross sections for e^+e^- annihilation into $J/\psi\eta_c$ and other double-charmonium states such as $J/\psi\chi_{cJ}$ $(J = 0, 1, 2)$ will be useful to clarify the problem. Experimentally, aside from $e^+ + e^- \to J/\psi + \chi_{c0}$ [2], Belle [10] has also studied processes $e^+ + e^- \to \chi_{c1} + X$ and $e^+ + e^- \to \chi_{c2} + X$, so we hope that the double-charmonium production involving χ_{cJ} $(J = 0, 1, 2)$ will be detectable in the near future. In the following we will calculate the cross sections $\sigma(e^+ + e^- \to J/\psi + \eta_c)$ and $\sigma(e^+ + e^- \to J/\psi + \chi_{cJ})$ in the leading order perturbative QCD. To this order ($\sim \alpha_s^2$) the color-singlet channel is dominant since all color-octet channels are of high order of v, which is the relative velocity of the charm quark and anti-charm quark in the charmonium, and therefore suppressed relative to the color-singlet channel (the relative suppression is at least of order v^4 for the cross sections). Furthermore, in order to compare exclusive production with inclusive production rates associated with the χ_{cJ} charmonium states, we will calculate the cross section $\sigma(e^+ + e^- \to \chi_{c0} + c\bar{c})$, and hope these ratios will be useful for both inclusive and exclusive production analyses at $\sqrt{s} = 10.6$ GeV.

We now write down the scattering amplitude in the nonrelativistic approximation to describe the creation of two color-singlet $c\bar{c}$ pairs which subsequently hadronize to two charmonium states in the e^+e^- annihilation process in Fig. 1 as [11,12]

$$
\begin{aligned}
&\mathcal{A}\big(a+b\to Q\bar{Q}\big(^{2S_\psi+1}L_{J_\psi}\big)(p_3)+Q\bar{Q}\big(^{2S+1}L_J\big)(p_4)\big)\\
&\quad=\sqrt{C_{L_\psi}}\sqrt{C_L}\sum_{L_{\psi z}S_{\psi z}}\sum_{s_1s_2}\sum_{jk}\sum_{L_zS_z}\sum_{s_3s_4}\sum_{il}\langle s_1;s_2|S_\psi S_{\psi z}\rangle\langle L_\psi L_{\psi z};S_\psi S_{\psi z}|J_\psi J_{\psi z}\rangle\langle 3j;\bar{3}k|1\rangle\\
&\qquad\times\langle s_3;s_4|SS_z\rangle\langle LL_z;SS_z|JJ_z\rangle\langle 3l;\bar{3}i|1\rangle\\
&\qquad\times\begin{cases}\mathcal{A}(a+b\to Q_j(\frac{p_3}{2})+\bar{Q}_k(\frac{p_3}{2})+Q_l(\frac{p_4}{2})+\bar{Q}_i(\frac{p_4}{2})) & (L=S),\\ \epsilon^*_\alpha(L_Z)\mathcal{A}^\alpha(a+b\to Q_j(\frac{p_3}{2})+\bar{Q}_k(\frac{p_3}{2})+Q_l(\frac{p_4}{2})+\bar{Q}_i(\frac{p_4}{2})) & (L=P),\end{cases}
\end{aligned}
\tag{1}
$$

where $\langle 3j;\bar{3}k|1\rangle = \delta_{jk}/\sqrt{N_c}$, $\langle 3l;\bar{3}i|1\rangle = \delta_{li}/\sqrt{N_c}$, $\langle s_1;s_2|S_\psi S_{\psi z}\rangle$, $\langle s_3;s_4|SS_z\rangle$, $\langle L_\psi L_{\psi z};S_\psi S_{\psi z}|J_\psi J_{\psi z}\rangle$, and $\langle LL_z;SS_z|JJ_z\rangle$ are, respectively, the color-SU(3), spin-SU(2), and angular momentum Clebsch–Gordan

coefficients for $Q\overline{Q}$ pairs projecting out appropriate bound states. $\mathcal{A}(a+b\to Q_j(\frac{p_3}{2})+\overline{Q}_k(\frac{p_3}{2})+Q_l(\frac{p_4}{2})+\overline{Q}_i(\frac{p_4}{2}))$ is the scattering amplitude for double $Q\overline{Q}$ production and $\mathcal{A}^\alpha$ is the derivative of the amplitude with respect to the relative spacing between the quark and antiquark in the bound state. The coefficients C_{L_ψ} and C_L can be related to the radial wave function of the bound states or its derivative with respect to the relative momentum as

$$C_s=\frac{1}{4\pi}\big|R_s(0)\big|^2,\qquad C_p=\frac{3}{4\pi}\big|R'_p(0)\big|^2. \tag{2}$$

We introduce the spin projection operators $P_{SS_z}(p,q)$ as [11,12]

$$P_{SS_z}(p,q)\equiv\sum_{s_1s_2}\langle s_1;s_2|SS_z\rangle v\left(\frac{p}{2}-q;s_1\right)\bar{u}\left(\frac{p}{2}+q;s_2\right). \tag{3}$$

Expanding $P_{SS_z}(P,q)$ in terms of the relative momentum q, we get the projection operators and their derivatives, which will be used in our calculation, as follows

$$P_{1S_z}(p,0)=\frac{1}{2\sqrt{2}}\not{\epsilon}^*(S_z)(\not{p}+2m_c), \tag{4}$$

$$P_{00}(p,0)=\frac{1}{2\sqrt{2}}\gamma_5(\not{p}+2m_c), \tag{5}$$

$$P^\alpha_{1S_z}(p,0)=\frac{1}{4\sqrt{2}m_c}\big[\gamma^\alpha\not{\epsilon}^*(S_z)(\not{p}+2m_c)-(\not{p}-2m_c)\not{\epsilon}(S_z)\gamma^\alpha\big]. \tag{6}$$

Then one can calculate the cross sections for the on-shell quarks in the factorized form of NRQCD [1]. The cross section for $e^++e^-\to J/\psi+\eta_c$ process in Fig. 1 is given by

$$\sigma\big(a(p_1)+b(p_2)\to J/\psi(p_3)+\eta_c(p_4)\big)=\frac{2\pi\alpha^2\alpha_s^2|R_s(0)|^4\sqrt{s-16m_c^2}}{81m_c^2s^{3/2}}\int_{-1}^{1}|\overline{M}|^2\,d\cos\theta, \tag{7}$$

where θ is the scattering angle between $\vec{p}_1$ and $\vec{p}_3$, $|\overline{M}|^2$ is as follows

$$|\overline{M}|^2=\frac{16384m_c^2(t^2+u^2-32m_c^4)}{s^5}. \tag{8}$$

The Mandelstam variables are defined as

$$s=(p_1+p_2)^2, \tag{9}$$

$$t=(p_3-p_1)^2=4m_c^2-\frac{s}{2}\big(1-\sqrt{1-16m_c^2/s}\cos\theta\big), \tag{10}$$

$$u=(p_3-p_2)^2=4m_c^2-\frac{s}{2}\big(1+\sqrt{1-16m_c^2/s}\cos\theta\big). \tag{11}$$

The cross section for $e^++e^-\to J/\psi+\chi_{cJ}$ process is

$$\sigma\big(a(p_1)+b(p_2)\to J/\psi(p_3)+\chi_{cJ}(p_4)\big)=\frac{2\pi\alpha^2\alpha_s^2|R_s(0)|^2|R'_p(0)|^2\sqrt{s-16m_c^2}}{27m_c^2s^{3/2}}\int_{-1}^{1}|\overline{M}_J|^2\,d\cos\theta, \tag{12}$$

where $|\overline{M}_J|^2$ for χ_{c0}, χ_{c1}, and χ_{c2} are given by

$$|\overline{M}_0|^2 = 2048\big(90112m_c^{10} - 74752m_c^8 t - 74752m_c^8 u + 23360m_c^6 t^2 + 43136m_c^6 tu + 23360m_c^6 u^2 - 3152m_c^4 t^3 - 7600m_c^4 t^2 u - 7600m_c^4 tu^2 - 3152m_c^4 u^3 + 162m_c^2 t^4 + 444m_c^2 t^3 u + 564m_c^2 t^2 u^2 + 444m_c^2 tu^3 + 162m_c^2 u^4 - t^4 u - 3t^3 u^2 - 3t^2 u^3 - tu^4\big)\big/\big(3s^7 m_c^2\big), \tag{13}$$

$$|\overline{M}_1|^2 = 32768\big(1792m_c^8 + 256m_c^6 t + 256m_c^6 u - 56m_c^4 t^2 - 64m_c^4 tu - 56m_c^4 u^2 - 4m_c^2 t^3 - 20m_c^2 t^2 u - 20m_c^2 tu^2 - 4m_c^2 u^3 + t^4 + 2t^3 u + 2t^2 u^2 + 2tu^3 + u^4\big)\big/s^7, \tag{14}$$

$$|\overline{M}_2|^2 = 4096\big(145408m_c^{10} - 1024m_c^8 t - 1024m_c^8 u - 2368m_c^6 t^2 - 6400m_c^6 tu - 2368m_c^6 u^2 + 16m_c^4 t^3 - 208m_c^4 t^2 u - 208m_c^4 tu^2 + 16m_c^4 u^3 + 24m_c^2 t^4 + 72m_c^2 t^3 u + 96m_c^2 t^2 u^2 + 72m_c^2 tu^3 + 24m_c^2 u^4 - t^4 u - 3t^3 u^2 - 3t^2 u^3 - tu^4\big)\big/\big(3s^7 m_c^2\big). \tag{15}$$

In the numerical calculations, we choose $\sqrt{s} = 10.6$ GeV, $m_c = 1.5$ GeV, $\alpha_s = 0.26$, $|R_s(0)|^2 = 0.810$ GeV^3 and $|R'_p(0)|^2 = 0.075$ GeV^5 [13], and assume that in the nonrelativistic approximation $m_{J/\psi} = m_{\eta_c} = m_{\chi_{cJ}} = 2m_c$. The numerical result for $e^+ + e^- \to J/\psi + \eta_c$ is

$$\sigma\big(e^+ + e^- \to J/\psi + \eta_c\big) = 5.5 \text{ fb}. \tag{16}$$

While the numerical result for the cross section of $e^+ + e^- \to J/\psi + \eta_c$ is more than a factor of six smaller than the experimental data [2] (with uncertainties due to the unknown decay branching fractions into $\geqslant 4$-charged particles for the η_c), the calculated ratio of $\sigma(e^+ + e^- \to J/\psi + \eta_c)/\sigma(e^+ + e^- \to J/\psi + c\bar{c}) \approx 0.037$ might be consistent with the experimental result with the choice of $\sigma(e^+ + e^- \to J/\psi + c\bar{c}) = 148$ fb obtained by taking our input parameters.

The cross sections for $J/\psi\chi_{cJ}$ production at $\sqrt{s} = 10.6$ GeV are given as

$$\sigma\big(e^+ + e^- \to J/\psi + \chi_{c0}\big) = 6.7 \text{ fb}, \tag{17}$$

$$\sigma\big(e^+ + e^- \to J/\psi + \chi_{c1}\big) = 1.1 \text{ fb}, \tag{18}$$

$$\sigma\big(e^+ + e^- \to J/\psi + \chi_{c2}\big) = 1.6 \text{ fb}. \tag{19}$$

In Fig. 2, we show the cross sections as functions of the e^+e^- center-of-mass energy $\sqrt{s}$, and we can see that the cross sections for $e^+ + e^- \to J/\psi + \eta_c$, $e^+ + e^- \to J/\psi + \chi_{c1}$ and $e^+ + e^- \to J/\psi + \chi_{c2}$ decrease rapidly as $\sqrt{s}$ increases. But the one with $J/\psi + \chi_{c2}$ decreases more slowly than that with $J/\psi + \eta_c$ and $J/\psi + \chi_{c1}$.

At $\sqrt{s} = 10.6$ GeV if we choose $\sigma(e^+ + e^- \to \chi_{c1} + c\bar{c}) = 18.1$ fb and $\sigma(e^+ + e^- \to \chi_{c2} + c\bar{c}) = 8.4$ fb which were obtained in the fragmentation approximation in Ref. [14], then we have the ratios

$$\frac{\sigma(e^+ + e^- \to J/\psi + \chi_{c1})}{\sigma(e^+ + e^- \to \chi_{c1} + c\bar{c})} = 0.061, \tag{20}$$

$$\frac{\sigma(e^+ + e^- \to J/\psi + \chi_{c2})}{\sigma(e^+ + e^- \to \chi_{c2} + c\bar{c})} = 0.19, \tag{21}$$

$$\frac{\sigma(e^+ + e^- \to J/\psi + \chi_{c1})}{\sigma(e^+ + e^- \to J/\psi + c\bar{c})} = 0.007, \tag{22}$$

$$\frac{\sigma(e^+ + e^- \to J/\psi + \chi_{c2})}{\sigma(e^+ + e^- \to J/\psi + c\bar{c})} = 0.011. \tag{23}$$

As for the χ_{c0} inclusive double-charm production the rate was not given in Ref. [14], we calculate $\sigma(e^+ + e^- \to \chi_{c0} + c\bar{c})$ in a complete form to the $\mathcal{O}(\alpha_s^2)$ order in perturbative QCD.

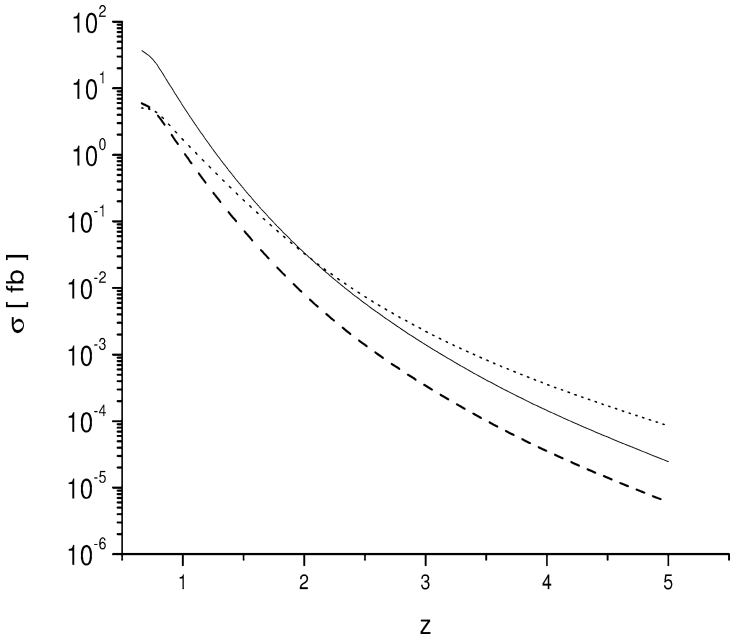

Fig. 2. Cross sections for $\sigma(e^+ + e^- \to J/\psi + \eta_c)$ (solid line) and $\sigma(e^+ + e^- \to J/\psi + \chi_{cJ})$ (dashed line for $J = 1$, dotted line for $J = 2$) plotted against the e^+e^- center-of-mass energy $\sqrt{s}$ with $z = \sqrt{s/s_0}$ and $\sqrt{s_0} = 10.6$ GeV.

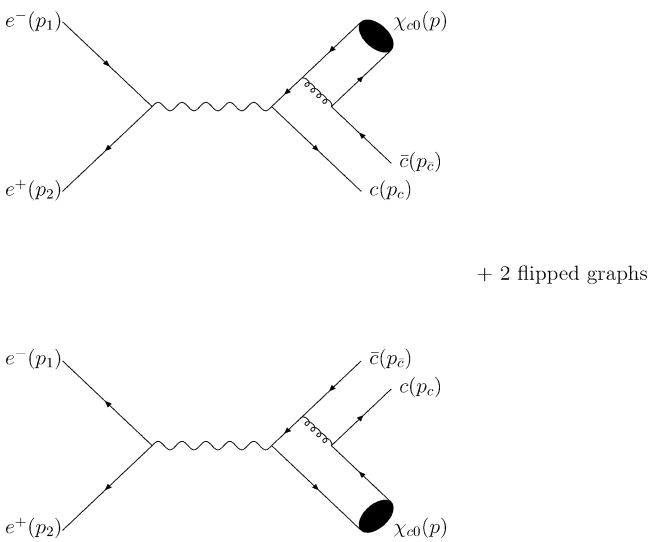

Fig. 3. Feynman diagrams for $e^+ + e^- \to \chi_{c0} + c\bar{c}$ process.

We give the amplitude of the first diagram in Fig. 3 for $e^+ + e^- \to \chi_{c0} + c\bar{c}$ as

$$M = \sum_{L_z S_z} \epsilon^*_\sigma(L_z)\langle 1L_z; 1S_z|J=0, J_z=0\rangle \sqrt{C_L}\, \frac{ie_c e g_s^2 [T^a T^a]_{li}}{\sqrt{3}} \bar{v}(p_2)\gamma^\mu u(p_1)\frac{1}{s}\bar{u}_l(p_c) \times \left[\gamma^\alpha P_{1S_z}\gamma_\alpha \mathcal{O}^\sigma_\mu + \gamma^\alpha P^\sigma_{1S_z}\gamma_\alpha \mathcal{O}_\mu\right] v_i(p_{\bar{c}}), \tag{24}$$

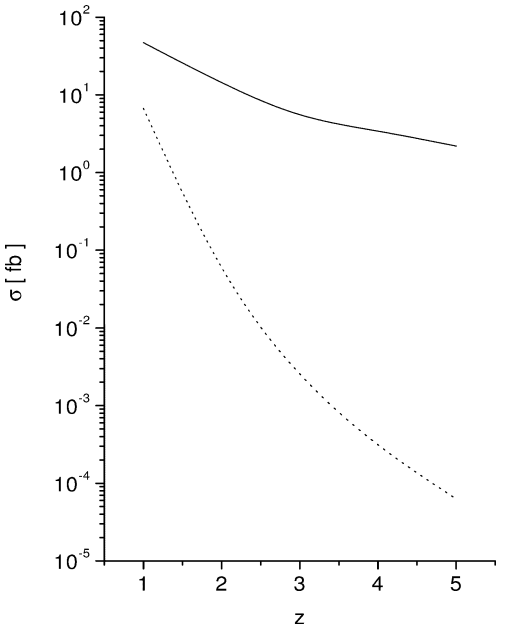

Fig. 4. Cross sections for $\sigma(e^+ + e^- \to \chi_{c0} + c\bar{c})$ (solid line) and $\sigma(e^+ + e^- \to J/\psi + \chi_{c0})$ (dotted line) plotted against the e^+e^- center-of-mass energy $\sqrt{s}$ with $z = \sqrt{s/s_0}$ and $\sqrt{s_0} = 10.6$ GeV.

where $e_c = (2/3)e$, T^a is the SU(3) color matrix, the matrix $\mathcal{O}_\mu$ is relevant to the on shell amplitude and $\mathcal{O}_\mu^\sigma$ is its derivative with respect to the relative momentum between the quarks that form the bound state. We can also express the contributions of other three diagrams in a similar way, and our numerical results are obtained with the full contributions of these four diagrams. Some useful information of the calculation is given in Appendix A.

We finally get the cross section for this process

$$\sigma\left(e^+ + e^- \to \chi_{c0} + c\bar{c}\right) = 49 \text{ fb}. \tag{25}$$

Then one has the ratio

$$\frac{\sigma(e^+ + e^- \to J/\psi + \chi_{c0})}{\sigma(e^+ + e^- \to \chi_{c0} + c\bar{c})} = 0.14, \tag{26}$$

$$\frac{\sigma(e^+ + e^- \to J/\psi + \chi_{c0})}{\sigma(e^+ + e^- \to J/\psi + c\bar{c})} = 0.045. \tag{27}$$

In Fig. 4, we show cross sections for $\sigma(e^+ + e^- \to \chi_{c0} + c\bar{c})$ (solid line) and $\sigma(e^+ + e^- \to J/\psi + \chi_{c0})$ (dotted line) plotted against the e^+e^- center-of-mass energy $\sqrt{s}$ with $z = \sqrt{s/s_0}$ and $\sqrt{s_0} = 10.6$ GeV. One can see the ratio in Eq. (26) decreases drastically as the center-of-mass energy increases. This is consistent with the result in Fig. 2. We hope the ratios between Eqs. (20) and (27) could be tested in the near future.

In summary, despite of many uncertainties due to the relativistic corrections, the QCD radiative corrections, the possible color-octet channel contributions, and the choice of physical parameters (e.g., the charm quark mass and the strong coupling constant), both the inclusive and exclusive double charm production cross sections calculated in perturbative QCD turned out to be seriously underestimated as compared with data. Therefore we intend to conclude, as in [3], that it seems hard to explain the double charm production data observed by Belle based on perturbative QCD (including both color-singlet and color-octet channels), and possible nonperturbative QCD effects should be considered at $\sqrt{s} = 10.6$ GeV.

While we were about to submit our result, there appeared one paper which also considered exclusive double-charmonium production [15]. Those authors took the QED effects into account in addition to the QCD effects that we considered. We find our result for the exclusive double-charmonium production is consistent with theirs but we also analyzed some inclusive processes which were not discussed in Ref. [15].

Acknowledgements

The authors thank L.K. Hao and Z.Z. Song for useful discussions. We also thank C.F. Qiao for helpful comments. This work was supported in part by the National Natural Science Foundation of China, and the Education Ministry of China.

Appendix A

In this appendix we give the cross section for the $e^+ + e^- \to \chi_{c0} + c\bar{c}$ process shown in Fig. 3.

$$d\sigma = \frac{|\overline{M}|^2}{2s(2\pi)^5}\delta^4(p_1 + p_2 - p_c - p_{\bar{c}} - p)\,\frac{d^3p_c}{2E_c}\,\frac{d^3p_{\bar{c}}}{2E_{\bar{c}}}\,\frac{d^3p}{2E}. \tag{A.1}$$

It is convenient to rewrite the cross section as

$$\begin{aligned} d\sigma &= \frac{|\overline{M}|^2}{2s(2\pi)^5}\delta^4(p_1 + p_2 - \eta - p)\delta^4(\eta - p_c - p_{\bar{c}})\,\frac{d^3p_c}{2E_c}\,\frac{d^3p_{\bar{c}}}{2E_{\bar{c}}}\,\frac{d^3p}{2E}\,d^4\eta \\ &= \frac{|\overline{M}|^2}{2s(2\pi)^5}\delta^4(p_1 + p_2 - \eta - p)\delta^4(\eta - p_c - p_{\bar{c}})\,\frac{d^3p_c}{2E_c}\,\frac{d^3p_{\bar{c}}}{2E_{\bar{c}}}\,\frac{d^3p}{2E}\,\frac{d^3\eta}{2E_\eta}\,dm_\eta^2, \end{aligned} \tag{A.2}$$

where $m_\eta^2 = \eta^2$.

The integral over the phase–space of $c\bar{c}$ is evaluated in the corresponding center-of-mass frame

$$\frac{d^3p_c'}{2E_c'}\,\frac{d^3p_{\bar{c}}'}{2E_{\bar{c}}'}\,\delta^4\big(\eta' - p_c' - p_{\bar{c}}'\big) = \frac{1}{8m_\eta^2}\lambda^{1/2}\big(m_\eta^2, m_c^2, m_c^2\big)\,d\Omega', \tag{A.3}$$

where $\lambda(a^2, b^2, c^2) = a^4 + b^4 + c^4 - 2a^2b^2 - 2a^2c^2 - 2b^2c^2$.

The remaining integration are performed in the e^+e^- center-of-mass frame

$$\frac{d^3p}{2E}\,\frac{d^3\eta}{2E_\eta}\,\delta^4(p_1 + p_2 - \eta - p) = \frac{1}{8s}\lambda^{1/2}\big(s, m_\eta^2, m_p^2\big)\,d\Omega, \tag{A.4}$$

where $m_p = 2m_c$, is the mass of the bound state.

Finally we have

$$d\sigma = \frac{|\overline{M}|^2 C_P}{64s^2(2\pi)^5 m_\eta m_c}\lambda^{1/2}\big(m_\eta^2, m_c^2, m_c^2\big)\lambda^{1/2}\big(s, m_\eta^2, m_p^2\big)\,d\Omega'\,d\Omega\,dm_\eta. \tag{A.5}$$

The limit of m_η is

$$2m_c \leqslant m_\eta \leqslant \sqrt{s} - m_p. \tag{A.6}$$

To accomplish the integration we use the Lorentz transformation between the two frames as $L = R_2 R_1$, where

$$R_1 = \begin{pmatrix} \sqrt{1+\frac{\vec{p}^2}{m_\eta^2}} & 0 & 0 & -\frac{|\vec{p}|}{m_\eta} \\ 0 & 1 & 0 & 0 \\ 0 & 0 & 1 & 0 \\ -\frac{|\vec{p}|}{m_\eta} & 0 & 0 & \sqrt{1+\frac{\vec{p}^2}{m_\eta^2}} \end{pmatrix}, \tag{A.7}$$

$$R_2 = \begin{pmatrix} 1 & 0 & 0 & 0 \\ 0 & \cos\theta & 0 & \sin\theta \\ 0 & 0 & 1 & 0 \\ 0 & -\sin\theta & 0 & \cos\theta \end{pmatrix}. \tag{A.8}$$

The momenta in the e^+e^- center-of-mass frame are

$$p_1 = \left(\frac{\sqrt{s}}{2}, 0, 0, \frac{\sqrt{s}}{2}\right), \tag{A.9}$$

$$p_2 = \left(\frac{\sqrt{s}}{2}, 0, 0, -\frac{\sqrt{s}}{2}\right), \tag{A.10}$$

$$p_c = R_2 R_1 p_c', \tag{A.11}$$

$$p_{\bar{c}} = R_2 R_1 p_{\bar{c}}', \tag{A.12}$$

$$p = \left(\sqrt{\vec{p}^2 + m_p^2}, |\vec{p}|\sin\theta, 0, |\vec{p}|\cos\theta\right), \tag{A.13}$$

where p_c' and $p_{\bar{c}}'$ are the momenta of c and $\bar{c}$ in the Ω' frame, and they are

$$p_c' = \left(E_c', |\vec{p}_c'|\sin\theta'\cos\theta', |\vec{p}_c'|\sin\theta'\cos\theta', |\vec{p}_c'|\cos\theta'\right), \tag{A.14}$$

$$p_{\bar{c}}' = \left(E_{\bar{c}}', -|\vec{p}_c'|\sin\theta'\cos\theta', -|\vec{p}_c'|\sin\theta'\cos\theta', -|\vec{p}_c'|\cos\theta'\right). \tag{A.15}$$

In Fig. 3 the lower (nonfragmentation) diagrams give very small contributions (about 3 percent), so for simplicity here we only write down the expressions for the contribution of the upper diagrams and give

$$|\overline{M}|^2 = \frac{2(4\pi)^4\alpha^2\alpha_s^2}{27}(aa + 2ab + bb). \tag{A.16}$$

We define $pp_1 = p.p_1$, $pp_2 = p.p_2$, $pp_3 = p.p_c$, $pp_4 = p.p_{\bar{c}}$, $p_{13} = p_1.p_c$, $p_{14} = p_1.p_{\bar{c}}$, $p_{23} = p_2.p_c$, $p_{24} = p_2.p_{\bar{c}}$. We notify $aa = bb$ and

$$\begin{aligned} aa = {} & \big[4\big(800m_c^{10}s + 800m_c^8 p_{14}pp_2 + 800m_c^8 p_{24}pp_1 + 1440m_c^8 pp_3 s + 160m_c^6 p_{13}p_{24}pp_3 \\ & + 160m_c^6 p_{14}p_{23}pp_3 + 1440m_c^6 p_{14}pp_2 pp_3 + 1440m_c^6 p_{24}pp_1 pp_3 + 900m_c^6 pp_3^2 s \\ & + 184m_c^4 p_{13}p_{24}pp_3^2 + 184m_c^4 p_{14}p_{23}pp_3^2 + 856m_c^4 p_{14}pp_2 pp_3^2 + 856m_c^4 p_{24}pp_1 pp_3^2 \\ & + 216m_c^4 pp_3^3 s + 56m_c^2 p_{13}p_{24}pp_3^3 + 56m_c^2 p_{14}p_{23}pp_3^3 + 168m_c^2 p_{14}pp_2 pp_3^3 \\ & + 168m_c^2 p_{24}pp_1 pp_3^3 + 13m_c^2 pp_3^4 s + 2p_{13}p_{24}pp_3^4 + 2p_{14}p_{23}pp_3^4\big)\big] \\ & \times \left[3m_c^2 s^2\left(64m_c^{12} + 192m_c^{10}pp_3 + 240m_c^8 pp_3^2 + 160m_c^6 pp_3^3 + 60m_c^4 pp_3^4 + 12m_c^2 pp_3^5 + pp_3^6\right)\right]^{-1}, \end{aligned} \tag{A.17}$$

$$
\begin{aligned}
ab = {} & \big[4\big(400m_c^{10}s + 400m_c^8 p_{13}pp_2 + 400m_c^8 p_{14}pp_2 + 400m_c^8 p_{23}pp_1 + 400m_c^8 p_{24}pp_1 \\
& + 400m_c^8 pp_1pp_2 + 480m_c^8 pp_3 s + 400m_c^8 pp_{34}s + 480m_c^8 pp_4 s + 80m_c^6 p_{13}p_{24}pp_3 \\
& + 80m_c^6 p_{13}p_{24}pp_4 + 280m_c^6 p_{13}pp_2pp_3 + 440m_c^6 p_{13}pp_2pp_4 + 80m_c^6 p_{14}p_{23}pp_3 \\
& + 80m_c^6 p_{14}p_{23}pp_4 + 440m_c^6 p_{14}pp_2pp_3 + 280m_c^6 p_{14}pp_2pp_4 + 280m_c^6 p_{23}pp_1pp_3 \\
& + 440m_c^6 p_{23}pp_1pp_4 + 440m_c^6 p_{24}pp_1pp_3 + 280m_c^6 p_{24}pp_1pp_4 + 240m_c^6 pp_1pp_2pp_3 \\
& - 400m_c^6 pp_1pp_2pp_{34} + 240m_c^6 pp_1pp_2pp_4 + 140m_c^6 pp_3^2 s + 240m_c^6 pp_3pp_{34}s \\
& + 476m_c^6 pp_3pp_4 s + 240m_c^6 pp_{34}pp_4 s + 140m_c^6 pp_4^2 s + 40m_c^4 p_{13}p_{24}pp_3^2 + 104m_c^4 p_{13}p_{24}pp_3pp_4 \\
& + 40m_c^4 p_{13}p_{24}pp_4^2 + 20m_c^4 p_{13}pp_2pp_3^2 + 288m_c^4 p_{13}pp_2pp_3pp_4 + 120m_c^4 p_{13}pp_2pp_4^2 \\
& + 40m_c^4 p_{14}p_{23}pp_3^2 + 104m_c^4 p_{14}p_{23}pp_3pp_4 + 40m_c^4 p_{14}p_{23}pp_4^2 + 120m_c^4 p_{14}pp_2pp_3^2 \\
& + 288m_c^4 p_{14}pp_2pp_3pp_4 + 20m_c^4 p_{14}pp_2pp_4^2 + 20m_c^4 p_{23}pp_1pp_3^2 + 288m_c^4 p_{23}pp_1pp_3pp_4 \\
& + 120m_c^4 p_{23}pp_1pp_4^2 + 120m_c^4 p_{24}pp_1pp_3^2 + 288m_c^4 p_{24}pp_1pp_3pp_4 + 20m_c^4 p_{24}pp_1pp_4^2 \\
& - 240m_c^4 pp_1pp_2pp_3pp_{34} + 144m_c^4 pp_1pp_2pp_3pp_4 - 240m_c^4 pp_1pp_2pp_{34}pp_4 + 108m_c^4 pp_3^2 pp_4 s \\
& + 144m_c^4 pp_3pp_{34}pp_4 s + 108m_c^4 pp_3pp_4^2 s + 28m_c^2 p_{13}p_{24}pp_3^2 pp_4 + 28m_c^2 p_{13}p_{24}pp_3pp_4^2 \\
& + 12m_c^2 p_{13}pp_2pp_3^2 pp_4 + 72m_c^2 p_{13}pp_2pp_3pp_4^2 + 28m_c^2 p_{14}p_{23}pp_3^2 pp_4 + 28m_c^2 p_{14}p_{23}pp_3pp_4^2 \\
& + 72m_c^2 p_{14}pp_2pp_3^2 pp_4 + 12m_c^2 p_{14}pp_2pp_3pp_4^2 + 12m_c^2 p_{23}pp_1pp_3^2 pp_4 + 72m_c^2 p_{23}pp_1pp_3pp_4^2 \\
& + 72m_c^2 p_{24}pp_1pp_3^2 pp_4 + 12m_c^2 p_{24}pp_1pp_3pp_4^2 - 144m_c^2 pp_1pp_2pp_3pp_{34}pp_4 + 13m_c^2 pp_3^2 pp_4^2 s \\
& + 2p_{13}p_{24}pp_3^2 pp_4^2 + 2p_{14}p_{23}pp_3^2 pp_4^2\big)\big] \\
\times {} & \big[3m_c^2 s^2\big(64m_c^{12} + 96m_c^{10}pp_3 + 96m_c^{10}pp_4 + 48m_c^8 pp_3^2 + 144m_c^8 pp_3pp_4 + 48m_c^8 pp_4^2 + 8m_c^6 pp_3^3 \\
& + 72m_c^6 pp_3^2 pp_4 + 72m_c^6 pp_3pp_4^2 + 8m_c^6 pp_4^3 + 12m_c^4 pp_3^3 pp_4 + 36m_c^4 pp_3^2 pp_4^2 \\
& + 12m_c^4 pp_3pp_4^3 + 6m_c^2 pp_3^3 pp_4^2 + 6m_c^2 pp_3^2 pp_4^3 + pp_3^3 pp_4^3\big)\big]^{-1}. \qquad \text{(A.18)}
\end{aligned}
$$

References

[1] G.T. Bodwin, L. Braaten, G.P. Lepage, Phys. Rev. D 51 (1995) 1125.
[2] Belle Collaboration, K. Abe, et al., Phys. Rev. Lett. 89 (2002) 142001, hep-ex/0205104.
[3] K.T. Chao, L.K. Hao, hep-ph/0209189.
[4] G.L. Kane, J.P. Leveille, D.M. Scott, Phys. Lett. B 85 (1979) 115.
[5] S.J. Brodsky, C.R. Ji, Phys. Rev. Lett. 55 (1985) 2257.
[6] P. Cho, A.K. Leibovich, Phys. Rev. D 54 (1996) 6690.
[7] F. Yuan, C.F. Qiao, K.T. Chao, Phys. Rev. D 56 (1997) 321;
F. Yuan, C.F. Qiao, K.T. Chao, Phys. Rev. D 56 (1997) 1663.
[8] S. Baek, P. Ko, J. Lee, H.S. Song, J. Kor. Phys. Soc. 33 (1998) 97, hep-ph/9804455.
[9] V.V. Kiselev, A.K. Likhoded, M.V. Shevlyagin, Phys. Lett. B 332 (1994) 411.
[10] Belle Collaboration, K. Abe, et al., Phys. Rev. Lett. 88 (2002) 052001.
[11] P. Cho, A.K. Leibovich, Phys. Rev. D 53 (1996) 150;
P. Cho, A.K. Leibovich, Phys. Rev. D 53 (1996) 6203;
P. Ko, J. Lee, H.S. Song, Phys. Rev. D 54 (1996) 4312;
P. Ko, J. Lee, H.S. Song, Phys. Rev. D 60 (1999) 119902.
[12] J.H. Kühn, J. Kaolan, E.G.O. Safiani, Nucl. Phys. B 157 (1979) 125;
B. Guberina, J.H. Kühn, R.D. Peccei, R. Rückl, Nucl. Phys. B 174 (1980) 317.

[13] E.J. Eichten, C. Quigg, Phys. Rev. D 52 (1995) 1726.
[14] G.A. Schuler, M. Vänttinen, Phys. Rev. D 58 (1998) 017502.
[15] E. Braaten, J. Lee, hep-ph/0211085.